

# Grid Quality Enhancement via Direct Power Control in Photovoltaic-Integrated Energy Systems

Layate Zakaria<sup>1</sup>, Bahi Tahar<sup>2</sup>, Lekhchine Salima<sup>3</sup>

Submitted: 08/10/2024

Revised: 22/02/2025

Accepted: 11/03/2025

**Abstract:** This paper introduces a Direct Power Control (DPC)-based strategy designed to enhance power quality in grid-connected photovoltaic (PV) systems. The proposed system architecture incorporates a DC/DC boost converter alongside a three-phase inverter, ensuring efficient energy transfer and effective grid interaction. To maximize energy extraction from the PV array, the Perturb and Observe (P&O) algorithm is employed for Maximum Power Point Tracking (MPPT), enabling optimal performance under varying environmental conditions. The DPC methodology directly regulates instantaneous active and reactive power, achieving unity power factor (UPF) operation by maintaining reactive power at zero. The control strategy employs rotating coordinate transformations and precise grid voltage phase tracking, resulting in robust synchronization and improved dynamic behavior. To further simplify the design and improve the grid performances, an LCL filtering stage has been introduced in this work. Hence, the proposed approach demonstrates significant robustness against load disturbances and variability in operating conditions. Through detailed simulations, the system's performance is validated, showcasing its ability to enhance grid quality, maintain stability, and ensure seamless operation during both transient and steady-state scenarios. The results emphasize the potential of this DPC-based control strategy as an efficient, reliable, and scalable solution for improving grid power quality in PV-integrated energy systems.

**Keywords:** DPC, Electric grid, MPPT optimization, Phase Locked Loop, Photovoltaic, UPF.

## 1. Introduction

The increasing global demand for energy, coupled with the urgent need to address environmental sustainability, has brought renewable energy sources to the forefront of modern innovation. Among these, solar energy stands out for its reliability, minimal maintenance requirements, and extended service life. In particular, photovoltaic (PV) systems have emerged as a transformative solution to meet the dual objectives of energy security and environmental protection [1]. Recent advancements in technology and supportive global policies aimed at mitigating climate change have amplified the adoption of PV systems, solidifying their role as key contributors to the transition

toward clean energy. PV is expected to triple within the next two decades, reflecting its pivotal role in global energy strategies [2]. As energy consumption continues to serve as a fundamental indicator of industrial and societal progress, the growing need for sustainable power sources becomes increasingly critical. By harnessing the inexhaustible potential of solar energy, PV offer a sustainable pathway to address the pressing challenges of rising energy demands

and ecological preservation [3]-[4].

One of the most compelling applications of photovoltaic technology are the grid-connected systems using photovoltaics (PV) have appeared as a pivotal solution in the transition toward renewable energy, leveraging solar power to satisfy the increasing demand for hygienic and sustainable electricity [5]. These systems operate by converting sunlight into direct current (DC) power through solar panels, which is then transformed into alternating current (AC) by an inverter to ensure compatibility with the existing electrical grid. The seamless integration of PV systems into the grid not only allows for the efficient distribution of generated power but also eliminates the need for extensive energy storage infrastructure, making them more cost-effective and practical for widespread adoption [6]. Among their numerous advantages, grid-connected

<sup>1</sup> Doctor, Department of Electrical Engineering, Faculty Sciences and Technologies, Khemis Miliana University – 44001, Algeria.

Corresponding Author Email: [z.layate@univ-dbk.m.dz](mailto:z.layate@univ-dbk.m.dz);

ORCID ID: 0000-0003-3993-3951

<sup>2</sup> Professor, Department of Electrical Engineering, Faculty of Technologie, LASA Laboratory, Badji Mokhtar-Annaba University, 23000, Algeria. Email: [tahar.bahi@univ-annaba.dz](mailto:tahar.bahi@univ-annaba.dz), ORCID ID: 0000-0001-6822-2492

<sup>3</sup> Doctor, Department of Electrical Engineering, Faculty of Technologie, LGMM Laboratory, University 20 August 1955 Skikda -Algeria. Email: [s.lekhchine@univ-skikda.dz](mailto:s.lekhchine@univ-skikda.dz); ORCID ID: 0000-0002-4509-5838

PV systems can considerably lower greenhouse gas emissions and improve energy security, and stabilizing electricity costs. Additionally, They make bidirectional power flow possible, allowing surplus energy produced during the hottest parts of the day to be returned to the grid, further optimizing resource utilization. By harnessing the inexhaustible potential of solar energy, these systems indicate

a transformative step toward achieving a more sustainable and resilient energy future [7].

Besides that, Maximum Power Point Tracking (MPPT) has become a critical focus in modern photovoltaic (PV) applications to address the inherent challenges posed by the high cost of solar cells, their relatively low efficiency, and the variability of power output under changing environmental circumstances [8]. Among the diverse MPPT strategies, the method of P&O is distinguished by its simplicity and efficacy in enhancing photovoltaic system performance.

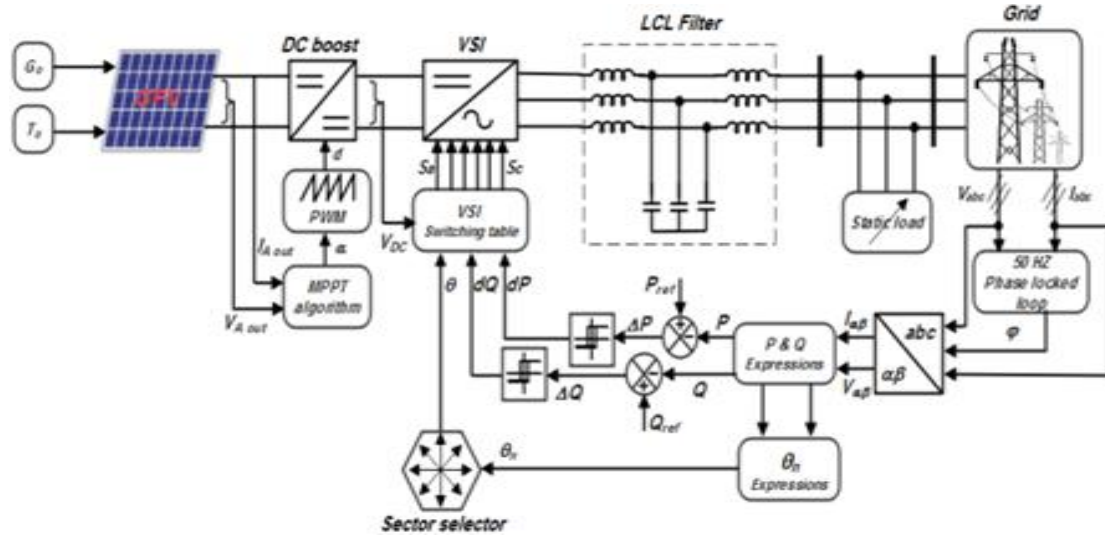


**Fig. 1. Global control system configuration**

Given the nonlinear behavior of PV modules under fluctuating temperature and irradiance, the algorithm of P&O plays an essential role in guaranteeing the constant extraction of maximum available power [9]. By dynamically adjusting the operating point of the PV array through iterative perturbation and evaluation, this algorithm enables real-time tracking of the peak power point. This process not only enhances the overall efficiency of PV systems but also contributes significantly to the effective utilization of renewable energy resources. As a result, P&O-based MPPT control has proven to be a robust and reliable approach, ensuring seamless integration of solar energy into modern energy infrastructures while maximizing its economic and ecological benefits [10].

Moreover, in Voltage Source Inverters (VSIs), three-phase grid-connected PV systems and Phase-Locked Loops (PLLs) serve as indispensable components that bridge the gap between efficient power generation and seamless grid integration. Building upon the effectiveness of MPPT algorithms, which ensure optimal energy extraction under varying environmental conditions, VSIs take charge of converting the DC output current from the PV array into AC current that aligns

with grid requirements [11]. This conversion is performed with high precision, minimizing harmonic distortion and ensuring stable operation even during dynamic and static load changes. The PLL complements this functionality by facilitating accurate synchronization of the photovoltaic system with the grid by monitoring the phase angle, frequency, and amplitude of the grid voltage in real time. This synchronization is critical for ensuring smooth power exchange, maintaining stability, and preventing disturbances in the grid [12]. Together, the VSI and PLL improves the overall efficiency and dependability of the system, making them crucial for the successful deployment of grid-connected photovoltaic systems.

Otherwise, for active and reactive power improvement, many control strategies were used in literature [13]-[14]-[15]. In this paper, we have employed the DPC technique. The method is based on the VSI commutation states generating where the objective is selecting the appropriate voltage vector to be applied on the VSI semi-conductors gates to ensure best performances in term of quickness response and stability of the utility grid by regulating the DC bus voltage at VSI input to manage both active and reactive power flows

under nature's imposed climatic conditions.

## 2. System overview

The studied conversion chain consists of several key components working in harmony to efficiently integrate photovoltaic (PV) energy into the grid. At its core, the system features a photovoltaic generator (PVG) coupled with a boost converter, which is regulated by an optimal MPPT algorithm. This ensures the extraction of the maximum power from the PVG under varying environmental conditions. A pulse-width modulation (PWM) block generates the duty cycle ( $\alpha$ ), which serves as the control signal for the semiconductor switch ( $K$ ) of the boost converter. The filtered output of the boost converter is then utilized to drive the three-phase inverter, which is connected to the grid through an LCL filter, ensuring smooth energy transfer and reduced harmonic distortion. The operation of the three-phase inverter is precisely managed by a DPC block, enabling robust regulation of active and reactive power. Figure 1 illustrates the overall architecture of the system under study, showcasing the seamless integration and functionality of its components.

### 2.1. PV unit model

The mathematical model of PV units is a cornerstone for understanding and optimizing their performance, enabling accurate predictions of electrical behavior under varying environmental conditions. This model begins at the PV cell level, the fundamental building block of PV systems, and extends to the PV array, which comprises interconnected modules designed for large-scale energy production [16]. As depicted in figure 2, the PV cell is considered as a semiconductor device that converts sunlight into electrical energy through the photovoltaic effect. The equivalent circuit of a PV cell consists of a current source  $I_{ph}$  representing the photocurrent, a diode for the p-n junction, and resistive elements  $R_s$  (series resistance) and  $R_{sh}$  (shunt resistance) to account for losses. The output current  $I_{out}$  of the PV cell is given by [17]:

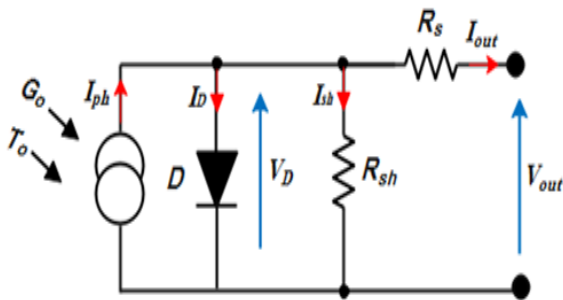


Fig. 2. Electrical PV cell equivalent scheme

$$I_{out} = I_{ph} - I_{DS} \left( e^{\frac{q V_D}{n k_B T_o}} - 1 \right) - \frac{V_D}{R_{sh}} \quad (1)$$

Where,  $V_{out}$  is the PV cell terminal voltage,  $I_{DS}$  the diode saturation current,  $q$  is the electron charge,  $V_D$  is the voltage across the diode given by  $V_D = V_{out} + I_{out} R_s$ . Also,  $n$  presents the diode ideality factor, typically comprises between 1 and 2. The  $k_B$  factor presents the Boltzmann constant and  $T_o$  is the cell operating temperature (in Kelvin).

### 2.2. DC-DC stage and MPPT control

The DC/DC conversion stage plays a critical role in PV systems by ensuring efficient energy transfer and voltage adaptation between the PV array and the grid-connected inverter [19]. In our study, a boost converter as shown in Figure 3 is used to elevate the output voltage of the PV array to the desired level, addressing the inherent variability in solar energy generation.

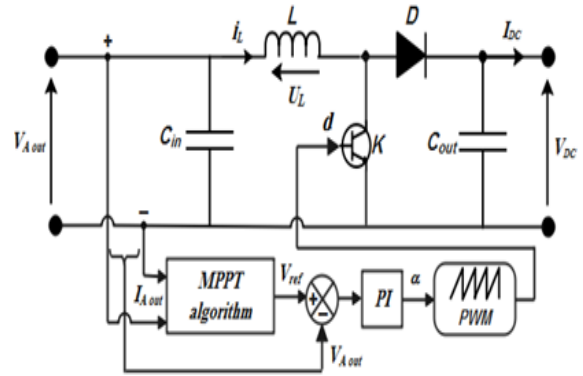


Fig. 3. DC/DC boost conversion stage

The dynamic behavior of the boost converter can be described using state-space equations derived from its operation in two modes, "switch ON" and "switch OFF". During the ON state, the inductor stores energy, while in the OFF state, the stored energy is transferred to the load via the diode. The voltage across the capacitor and the current through the inductor can be modelled as [20]:

$$\frac{dV_{DC}}{dt} = \frac{i_L(1-d) - I_{DC}}{C_{out}} \quad (2)$$

$$\frac{dI_{DC}}{dt} = \frac{V_{DC}(1-d) - V_{Aout}}{L} \quad (3)$$

### 2.3. MPPT control strategy

The P&O method optimizes the boost converter's performance by dynamically modifying the duty cycle  $d$  to sustain the maximum power point (MPP) of the photovoltaic array. This process involves perturbing

the operating point of the PV array and observing changes in its power output. If power increases, the perturbation continues in the same direction; if power decreases, the direction is reversed. This iterative adjustment ensures that the boost converter operates at the MPP, maximizing energy extraction from the PV array. Together, the mathematical model of the boost

converter and the P&O algorithm provide an efficient framework for achieving optimal power control in PV systems [21]. The below flowchart illustrating the operation of the P&O algorithm visually represents the iterative decision-making process, providing a clear understanding of its functionality and integration into the control of the DC boost bloc [22].

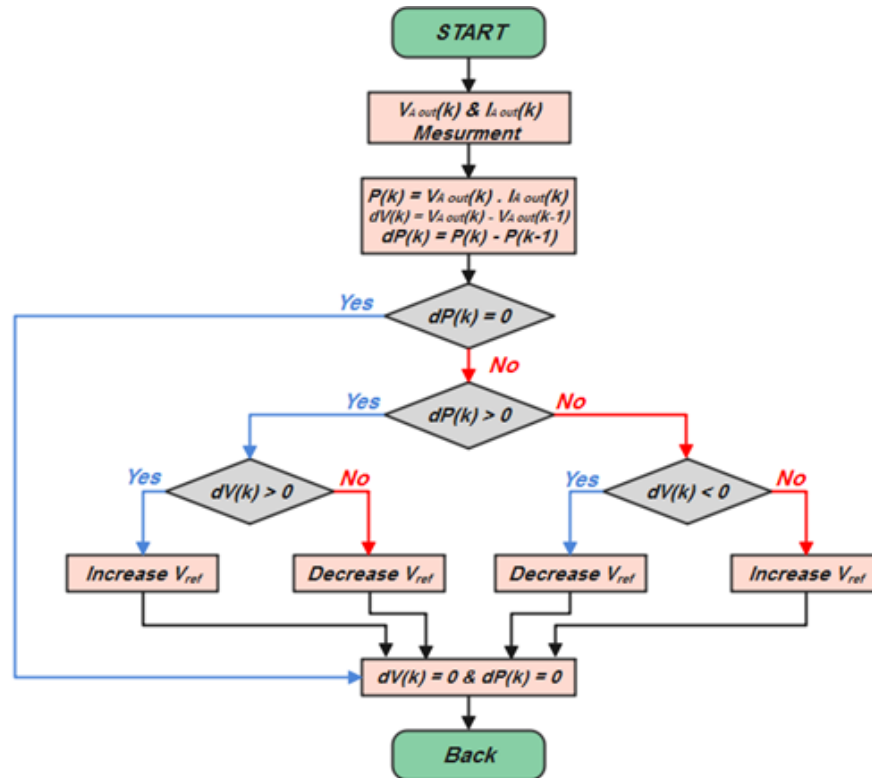


Fig. 4.MPPT flowchart control

3.

#### 4. Modeling of the voltage source inverter

Grid-connected systems refer to photovoltaic systems integrated into distribution nodes to supply electricity directly to the grid. This connection is facilitated through an inverter, which not only transforms the direct current (DC) produced by the solar panels into alternating current (AC) but also ensures synchronization with the grid in terms of voltage and frequency. These systems play a vital role in supporting energy distribution and maintaining seamless integration with existing electrical networks. The voltage source inverter is composed of three switching arms using insulated-gate bipolar transistors (IGBTs), where each arm consists of two cells. Each cell includes a diode and an IGBT connected in an anti-parallel configuration. All components are assumed to operate as ideal switches. The primary function of the three-phase inverter is to transfer power from the DC side to the grid.

The output of the inverter can produce two voltage levels based on the DC supply voltage and the states of the switches. The operation of the two switches within the same arm is complementary, meaning when one switch conducts, the other is blocked. The state of each switch is determined by control signals  $S_a$ ,  $S_b$ , and  $S_c$ . The eight possible output voltage states of the inverter are detailed in Table 1.

Table.1.VSI output generated voltages

Case N°	Sa	Sb	Sc	Va	Vb	Vc
1	0	0	0	0	0	0
2	0	0	1	$-V_{dc}/3$	$-V_{dc}/3$	$-V_{dc}/3$
3	0	1	0	$-V_{dc}/3$	$2*V_{dc}/3$	$-V_{dc}/3$
4	0	1	1	$-2*V_{dc}/3$	$V_{dc}/3$	$V_{dc}/3$

5	1	0	0	$2*V_{dc}/3$	$-V_{dc}/3$	$-V_{dc}/3$
6	1	0	1	$V_{dc}/3$	$2*V_{dc}/3$	$V_{dc}/3$
7	1	1	0	$V_{dc}/3$	$V_{dc}/3$	$V_{dc}/3$
8	1	1	1	0	0	0

## 5. Direct Power Control

(DPC) is an advanced power control approach strategy grounded in the theory of instantaneous power [23]-[24]. Its core principle involves selecting the optimal switching state for power semiconductors using a switching table combined with hysteresis comparisons. Specifically, the reference value for active power is derived from the output of the DC bus voltage regulator  $V_{DC}$ , while the reactive power reference is set to zero to ensure operation at a unity power factor.

Active power  $P$  is defined as the scalar product of voltage and current components, while reactive power  $Q$  is expressed as the vector product of same components.

$$\begin{cases} P = V_{\alpha}I_{\alpha} + V_{\beta}I_{\beta} \\ Q = V_{\alpha}I_{\beta} - V_{\beta}I_{\alpha} \end{cases} \quad (4)$$

Where,  $V_{\alpha}$ ,  $I_{\alpha}$ ,  $V_{\beta}$ , and  $I_{\beta}$  represent the Clarke components of the instantaneous values of three-phase voltages and currents.

The errors in active power ( $dP$ ) and reactive power ( $dQ$ ) are given by the following expressions [25]:

$$dP = P_{ref} - P \quad (5)$$

$$dQ = Q_{ref} - Q \quad (6)$$

Where  $P_{ref}$  represents the desired active of power,  $P$  the actual active of power,  $Q_{ref}$  desired reactive power, and  $Q$  the actual reactive power. Moreover, the angular of position  $\theta_n$  for the grid voltage vector is determined using the following formula:

$$\theta_n = \arctan\left(\frac{V_{\alpha}}{V_{\beta}}\right) \quad (7)$$

Where, in the case of field division into 12 sectors as shown in the figure, we have:

$$\frac{\pi}{6}(n-2) \leq (\theta_n - 1) \leq \frac{\pi}{6}(n-1) \quad (8)$$

$$n = 1, 2, 3, \dots, 12.$$

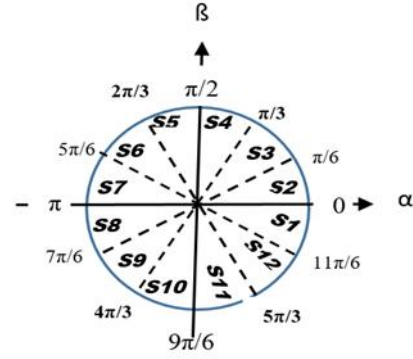


Fig. 5. Possible sectors selector

Using the error signals and the angular position, a switching table is constructed, storing all the switching states  $dP$  and  $dQ$  of the converter. These states take the value "1" to indicate an increase in the controlled variable ( $P$  or  $Q$ ) and "0" to indicate a decrease. The dual-level hysteresis regulators for instantaneous active and reactive power can be described as follows:

$$\begin{aligned} \text{If, } P_{ref} - P \geq HB_P \quad dP &= 1 \\ \text{If, } P_{ref} - P < HB_P \quad dP &= 0 \end{aligned} \quad (9)$$

The same for reactive power:

$$\begin{aligned} \text{If, } Q_{ref} - Q \geq HB_Q \quad dQ &= 1 \\ \text{If, } Q_{ref} - Q < HB_Q \quad dQ &= 0 \end{aligned} \quad (10)$$

However, the optimal switching states of the converter can be uniquely determined at any specific moment based on the combination of input signals, utilizing Table 2.

Table 2. VSI switching sectors

DP	DQ	SECTOR	VECTOR	SECTOR	VECTOR
1	0	S1	V6	S2	V7
	1		V7		V7
0	0	S3	V6	S4	V1
	1		V1		V2
1	0	S5	V1	S6	V1
	1		V0		V0
0	0	S7	V1	S8	V2
	1		V2		V3
1	0	S9	V2	S10	V7
	1		V7		V7
0	0	S11	V2	S12	V3
	1		V3		V4
1	0	S1	V3	S2	V0
	1		V0		V0
0	0	S3	V3	S4	V4
	1		V4		V5
1	0	S5	V4	S6	V7
	1		V7		V7
0	0	S7	V4	S8	V5
	1		V5		V6
1	0	S9	V5	S10	V0
	1		V0		V0
0	0	S11	V5	S12	V6
	1		V6		V1



## 5. Simulation results

In the context of analysing the conversion structure under study, we initially conducted a numerical simulation of the I-V ( $I_{pv} = f(V_{pv})$ ) and P-V ( $P_{pv} = f(V_{pv})$ ) characteristics of the photovoltaic generator (PVG), as illustrated in Table 3. This simulation was performed considering four levels of solar irradiance: 200 W/m<sup>2</sup>, 400 W/m<sup>2</sup>, 600 W/m<sup>2</sup>, and the standard reference level of 1000 W/m<sup>2</sup>. Consequently, Figure 6 presents the simulation results of these characteristics, while Table 4 records the associated characteristic values, including the irradiation level (G), the maximum voltage of the PVG ( $V_{pv\_max}$ ), the open-circuit current ( $I_{cc}$ ), and the maximum power ( $P_{pv\_max}$ ).

**Table 3. PV Parameters**

Parallel strings	3
Cells per module	60
Voltage at the peak power point (V)	29,3
Short-circuit current (A)	7,97
Maximum of Power (W)	218,871
Series-connected modules per string	7
Open circuit voltage (V)	36,6
Current at MPP (A)	7,47

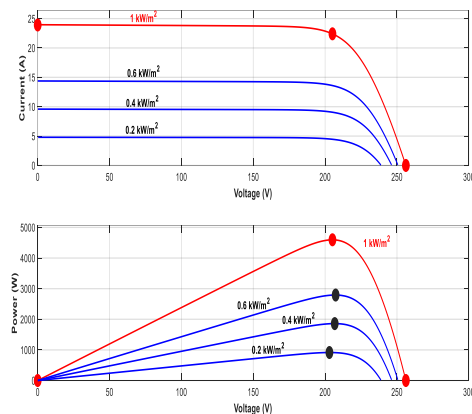


**Fig. 6. Characteristics of the photovoltaic generator of I-V and P-V**

**Table 4. Characteristics associated values of PVG, I-V and P-V**

$G(W/m^2)$	$V_{pv\_max}(V)$	$I_{cc}(A)$	$P_{pv\_max}(W)$
200	202,99	4,80	914,54

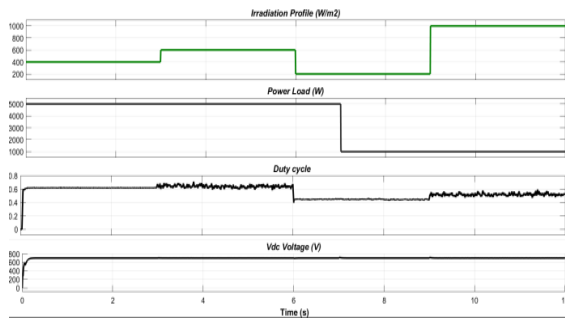
400	206,70	9,59	1859
600	207,31	14,38	2792
1000	205,1	23,91	4596

Subsequently, we analysed the overall operation of the system under standard temperature conditions (25°C) and a varying irradiation profile, as illustrated in Figure 7. The figure also demonstrates the required variable power levels and the evolution of the duty cycle controlling the field-effect transistor (IGBT) of the boost converter. It was observed that the duty cycle adjusts in accordance with changes in the irradiation level and remains within acceptable ranges. Moreover, the photovoltaic voltage waveform at the output of the boost converter is displayed at the bottom of this illustration. It is noted that the voltage consistently aligns with its reference value ( $V_{DC} = 700V$ ) set at the inverter input. However, each change in irradiation level causes a slight fluctuation in the voltage before it rapidly stabilizes at its desired value.

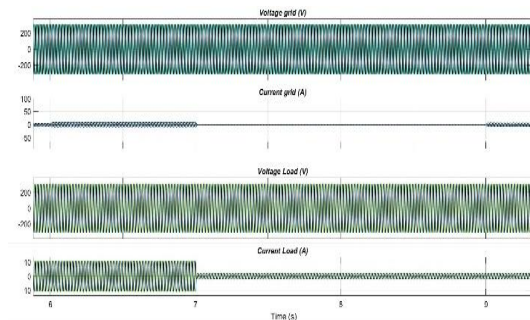
Figure 8 provides detailed enlargements of the voltage and current waveforms within the distribution network, as well as the voltage across the terminals of the variable load and the current flowing through it. The voltage remains sinusoidal and maintains fixed magnitudes, while the network currents fluctuate based on irradiation variations. Additionally, the currents passing through the load oscillate depending on the power demanded by the load. Under maximum load conditions ( $P = 5KW$  and  $Q = 1KW$ ), the current intensity can reach approximately 10A, while in reduced load scenarios, the current amplitude hovers around 2A.

The PV generator maintains a consistent power output, as depicted at the bottom of the graph, demonstrating that despite irradiation variations, the system operates at its maximum energy production capacity, as outlined in Table 2 through efficient MPPT management.

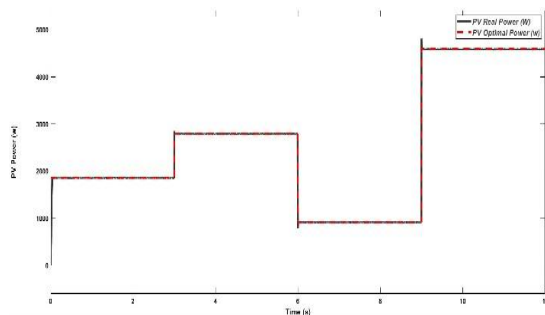
Furthermore, Figure 9 initially highlights the enlarged signals feeding into the DPC. This includes the hysteresis controller output for the active power component, the hysteresis controller output for the reactive power component, and the progression across the twelve corresponding sectors. The selection of the voltage vector at the inverter output is determined based on the switching table of the DPC (see Table 1) using these inputs and direct power control. The final data series confirms that the reactive and active power values precisely match their reference targets.



-a-



-b-



-c-

**Fig. 7. Input, control and output signals**

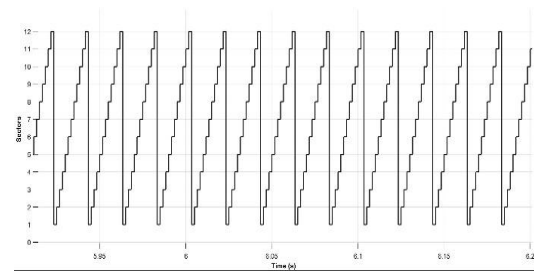
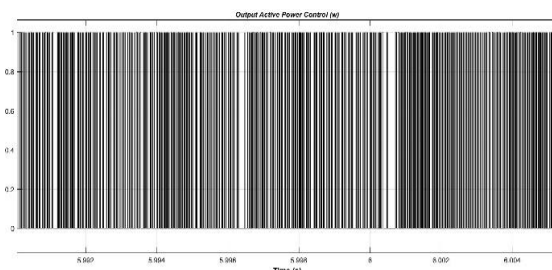
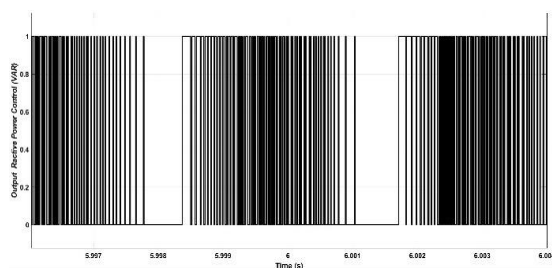


**Fig.8. a) Control signals of active and reactive power. b) DPC Sectors**

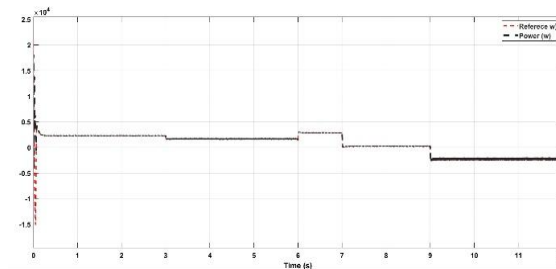
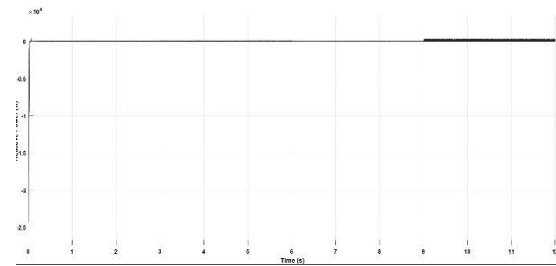
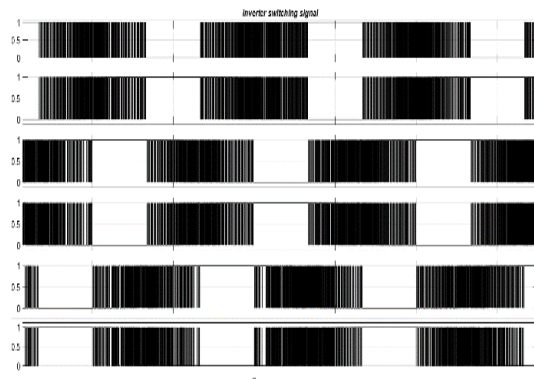


**Fig.9. Real and reference active and reactive power signals**

## 6. Conclusion

At the end of this work, it mainly contributes to the application of direct power control for a photovoltaic system connected to a distribution grid. It is found that the adopted approach ensures efficient management of active and reactive power while maintaining perfect regulation of the inverter input voltage regardless of climatic variations. The analysis of the results reveals that the considered control offers good control dynamics characterized by a rapid and precise response to variations in sunlight conditions or system loads as well as an adaptation of the operating point of

the photovoltaic generator to its maximum power. Furthermore, the control has proven to be a robust and efficient solution ensuring both performance, robustness and stability of the overall system

## References

- [1] Y. Che, S. Xue, and D. Wang, "An AC Voltage Sensor-less Control Strategy for Ocean Ship Photovoltaic Grid-connected Inverter with LCL Filter", *Journal of Coastal Research*, no. 83, p. 109-115, 2018.
- [2] A. Shawky, M. Ahmed, M. Orabi, and A.E. Aroudi, "Classification of three-phase grid-tied microinverters in photovoltaic applications", *Energies*, vol. 13, no. 11, pp. 2929, 2020.
- [3] M. Hosenuzzaman, N.A. Rahim, J. Selvaraj, M. Hasanuzzaman, A. A. Malek, and A. Nahar, "Global prospects, progress, policies, and environmental impact of solar photovoltaic power generation", *Renewable and sustainable energy reviews*, vol. 41, pp. 284-297, 2015.
- [4] N.K. John, C.C. Onwuagbu, and C.J. Chigozie, "Potential of integrated energy solution in Nigeria: opportunities and challenges for sustainable development-multi facet assessment model", *Discover Sustainability*, vol. 6, no. 1, pp. 1-19, 2025.
- [5] O. R. Alomar, N. M. Basher, O. M. Ali, A. Salih, N. M. Abdulrazzaq, and S. M. Samad, "Energetic, Economic Environmental Analysis for Photovoltaic Grid-Connected Systems under Different Climate Conditions in Iraq", *Cleaner Energy Systems*, vol. 10, pp. 100180, 2025.
- [6] J. Ma, C. Wang, Y. Cao, Z. Wu, C. Lu, K. Sun, C. Zhu, and X. Zhang, "Transient energy transfer of wind-photovoltaic-storage grid-connected system under virtual synchronous coupling", *Energy Reports*, vol. 12, pp. 4805-4812, 2024.
- [7] X. Zhang, Y. Chen, L. Cheng, S. Tian, and L. Liu, "PSO with segmented mutation for site selection in grid-connected photovoltaic power generation system", *Applied Energy*, vol. 377, pp. 124352, 2025.
- [8] S. Manna, D. K. Singh, A. K. Akella, H. Kotb, K. M. AboRas, H. M. Zawbaa, and S. Kamel, "Design and implementation of a new adaptive MPPT controller for solar PV systems", *Energy Reports*, vol. 9, pp. 1818-1829, 2023.
- [9] S. Motahhir, A. El Hammoumi, and A. El Ghzizal, "Photovoltaic system with quantitative comparative between an improved MPPT and existing INC and P&O methods under fast varying of solar irradiation", *Energy Reports*, vol. 4, pp. 341-350, 2018.
- [10] O. Turgut, "Global best algorithm based parameter identification of solar cell models. International Journal of Intelligent Systems and Applications in Engineering", vol. 5, no. 4, pp. 189-205, 2017.
- [11] F. Chakir, A. El Magri, M. Kissaoui, R. Lajouad, A. El Fadili, and M. Chakir, "Advanced control strategies for multilevel inverter in grid-connected and off-grid photovoltaic systems: A multi-objective approach using LS-PWM for THD reduction", *Scientific African*, vol. 26, pp. 1-21, 2024.
- [12] A. Sinha, K. C. Jana, and M. K. Das, "An inclusive review on different multi-level inverter topologies, their modulation and control strategies for a grid connected photo-voltaic system", *Solar Energy*, vol. 170, pp. 633-657, 2018.
- [13] Y. Zhao, A. An, Y. Xu, Q. Wang, and M. Wang, "Model predictive control of grid-connected PV power generation system considering optimal MPPT control of PV modules", *Protection and Control of Modern Power Systems*, vol. 6, pp. 1-12, 2021.
- [14] K. Y. Yap, C. M. Beh, and C. R. Sarimuthu, "Fuzzy logic controller-based synchronverter in grid-connected solar power system with adaptive damping factor", *Chinese Journal of Electrical Engineering*, vol. 7, no. 2, pp. 37-49, 2021.
- [15] Y. Yang, and H. Wen, "Adaptive perturb and observe maximum power point tracking with current predictive and decoupled power control for grid-connected photovoltaic inverters", *Journal of Modern Power Systems and Clean Energy*, vol. 7, no. 2, pp. 422-432, 2019.
- [16] A. Mansouri, A. El Magri, R. Lajouad, F. Giri, and A. Watil, "Optimization strategies and nonlinear control for hybrid renewable energy conversion system", *International Journal of Control, Automation and Systems*, vol. 21, no. 11, pp. 3796-3803, 2023.
- [17] Z. Layate, B. Tahar, and L. Salima, "Dynamic flow control of a photovoltaic pumping system-based asynchronous induction



- motor", *International Journal of Nonlinear Dynamics and Control*, vol. 1, no. 3, pp. 255-270, 2019.
- [18] K. El Mezdi, A. El Magri, A., Watil, I. El Myasse, L. Bahatti, R. Lajouad, and H. Ouabi, "Non-linear control design and stability analysis of hybrid grid-connected photovoltaic-Battery energy storage system with ANN-MPPT method", *Journal of Energy Storage*, vol. 72, pp. 108747, 2023.
  - [19] W. Alhosaini, M. Aly, E. M. Ahmed, and A. Shawky, "Optimized grid-connected three-phase photovoltaic inverter system using cascaded FO-PIT-FOPI fractional controller", *Energy Reports*, vol. 13, pp. 3324-3339, 2025.
  - [20] Z. Layate, T. Bahi, S. Lekhchine and M. Kaci, "Energy Management of Integrated Batteries in Grid-connected Photovoltaic System", *J. Electrical Systems*, vol. 21, no 1, pp. 102-115, 2025.
  - [21] J. J. Jijesh, "Comparative analysis of bio-inspired maximum power point tracking algorithms for solar photovoltaic applications", *International Journal of Intelligent Systems and Applications in Engineering*, vol. 11, no. 1, pp. 100-110, 2023.
  - [22] J. Sahoo, S. Samanta, and S. Bhattacharyya, "Adaptive PID controller with P&O MPPT algorithm for photovoltaic system", *IETE Journal of research*, vol. 66, no. 4, pp. 442-453, 2020.
  - [23] T. Ohnishi, "Three phase PWM converter/inverter by means of instantaneous active and reactive power control", In Proceedings IECON'9, *International Conference on Industrial Electronics, Control and Instrumentation, IEEE*, pp. 819-824, 1991.
  - [24] T. Noguchi, H. Tomiki, S. Kondo, and I. Takahashi, "Direct power control of PWM converter without power-source voltage sensors", *IEEE transactions on industry applications*, vol. 34, no. 3, pp. 473-479, 1998.
  - [25] J. Lamterkati, M. Khaffalah, and L. Ouboubker, "Fuzzy logic based improved direct power control of three-phase PWM rectifier", *International Conference on Electrical and Information Technologies, IEEE*, pp. 125-130, 2016.